Journal of Power Sources 213 (2012) 382–390

Contents lists available at SciVerse ScienceDirect

Journal of Power Sources

journal homepage: www.elsevier.com/locate/jpowsour

Porous anodes with helical flow pathways in bioelectrochemical systems: The effects of fluid dynamics and operating regimes

Jung Rae Kim [a], Hitesh C. Boghani [a], Negar Amini [b], Kondo-François Aguey-Zinsou [b,d], Iain Michie [a], Richard M. Dinsdale [c], Alan J. Guwy [c], Zheng Xiao Guo [b], Giuliano C. Premier [a,*]

[a] Sustainable Environment Research Centre (SERC), Faculty of Advanced Technology, University of Glamorgan, Pontypridd, Mid-Glamorgan CF37 1DL, UK
[b] Department of Chemistry, University of College London, London WC1H 0AJ, UK
[c] Sustainable Environment Research Centre (SERC), Faculty of Health, Sport and Science, University of Glamorgan, Pontypridd, Mid-Glamorgan CF37 1DL, UK
[d] School of Chemical Engineering, The University of New South Wales, Sydney NSW 2052, Australia

ARTICLE INFO

Article history:
Received 10 February 2012
Received in revised form
8 March 2012
Accepted 14 March 2012
Available online 7 April 2012

Keywords:
Microbial fuel cell (MFC)
Bioelectrochemical system (BES)
Helical electrode
Micro-porous carbon
Carbon foam
Flow induced mass transfer

ABSTRACT

Bioelectrochemical systems (BES) and/or microbial fuel cell (MFC) mass transport and associated overpotential limitations are affected by flow regimes, which may simultaneously increase the power and pollution treatment capacities. Two electrodes with helical flow channels were compared in the same tubular MFC reactor. 1). A machined monolithic microporous conductive carbon (MMCC). 2). A layered carbon veil with spoked ABS former (LVSF); both presented helical flow channel. Anode performances were compared when subject to temperature, substrate concentration and flow rate variations. The MMCC maximum power increased from 2.9 ± 0.3 to 7.6 ± 0.7 mW with influent acetate concentration, from 1 to 10 mM (with 2 mL min^{-1}), but decreased power to 5.5 ± 0.5 mW at 40 mM, implicated localized pH/buffering. Flow rate (0.1 to 7.5 mL min^{-1}) effects were relatively small but an increase was evident from batch to continuous operation at 0.1 mL min^{-1}. The LVSF configuration showed improved performance in power as the flow rate increased, indicating that flow pattern affects BES performance. Computational fluid dynamics (CFD) modelling showed less uniform flow with the LVSF. Thus flow regime driven mass transfer improves the power output in continuously fed system operation. These results indicate that electrode configuration, flow regime and operating condition need consideration to optimize the bioelectrochemical reaction.

1. Introduction

Bioelectrochemical systems (BES) have recently been extended to hydrogen and chemical production, desalination and bioremediation; all of which use bacterial electron transfer at an anode as a source of energy. BES, including microbial fuel cells (MFCs) and microbial electrolysis cells (MECs), use an electroactive biofilm located on an anode as a biocatalyst for converting biodegradable substrate to electricity, which may subsequently drive electrolysis for hydrogen production or other useful products and processes [1–3]. The anodes of MFCs, MECs and other BES are broadly similar and transferable in terms of electrogenesis from a biofilm.

Biofilm performance is improved by facilitating bacterial metabolism, yielding concomitant electrocatalysis. Improved catalysis can therefore be achieved by judicious process design and appropriate selection of operating conditions. The bioelectrochemical reaction is limited, though not exclusively; by mass transport processes, which for BES are most relevant at the interfaces between the bulk liquid, biofilm and electrode where the substrate oxidation and electron transfer to the solid electrode are catalysed by microorganisms. Thus the concentration gradients which develop at the electrode biofilm significantly affect biocatalytic activity and performance measures such as power production and organic removal rate. The mass transfer limitation in chemical fuel cells such as PEM fuel cells and solid oxide fuel cells has been studied extensively [4,5]. However in BES, there might be more significant effects because they have comparatively low power densities and are operated at room temperature, with fuels (substrates) provided in the bulk liquid

* Corresponding author. Tel.: +44 (0) 1443 482333; fax: +44 (0) 1443 482169.
E-mail address: gcpremier@glam.ac.uk (G.C. Premier).

0378-7753
doi:10.1016/j.jpowsour.2012.03.040

phase. Thus, large concentration gradients of the substrates may develop in the proximity of the biocatalyst on solid or porous electrodes.

Mass transport in the biofilm is mainly affected by temperature and the bulk concentrations of the substrates [6]. Fluid shear stress can reduce the film thickness over the biofilm and consequently can change the mass transport rate in the system [7–10]. Although BES have been initially tested in batch systems for proof of concept, it is frequently preferable to operate in continuous mode since the potential of bioelectrochemical system (BES) has often been focused on wastewater treatment system applications, with the prospect of simultaneous energy recovery; although other bioprocess applications are also important. A preferred system for wastewater treatment would have high flow rates with relatively low reactor volumes (low HRT) because such a system would have a lower reactor volume; lower capital, maintenance and possibly other operating costs [9]. Whilst operational temperature has been shown to have a direct influence on MFC performance [11]. Michie et al. [12] also demonstrated that temperature can influence the composition and level of biomass production on the electrode.

The high shear rates induced by high throughput could also increase mixing and substrate/media contact with bacteria and thus increase chemical oxygen demand (COD) removal rates. The fixed electrogenic biofilm on an anode in BES may have advantages in terms of its robustness against high shear rates, over the conventional treatment processes. Relatively high productivity or treatment capacity has been achieved in relatively small reactors with low HRT. Operating a BES in the continuous flow mode, presents hydrodynamic flow characteristics that may vary from laminar to turbulent at the electrode, depending on flow velocity, the characteristic dimensions, and surface roughness and shape of the flow channel and the fluid properties. In turn these parameters can influence the electrochemical performance of the BES and bacterial community development within them [7,13,14].

The physical and chemical characteristics of a porous anode electrode with a three-dimensional flow channel design could play an important role in providing a suitable surface for immobilizing a biofilm catalyst (of microorganisms) and a conductive electronic pathway to harvest electrical energy from electrogenic metabolic processes. Pores of micrometres in a carbon foam-like electrode material can provide favourable local environments for electrogenic bacterial attachment, which leads to high specific volumetric activity [10], whereas macro-porosities can facilitate substrate transport to inner surface regions to enhance total areas of contact. Carbon materials offer excellent affinity and bio-compatibility. Therefore, surface properties for enzyme/microbe immobilization can be tailored to increase performance. Moreover, porous carbon could also provide a balanced set of properties for various applications, such as low density, high electrical and thermal conductivities, high stability, and good corrosion resistance, which can be achieved at relatively low cost and are often not simultaneously available with other materials.

A number of researchers have also investigated three-dimensional anode electrode materials in MFCs such as granular graphite [15], carbon felt [16] and gas-assisted electrospinning carbon fibre nonwovens [17] which have demonstrated power densities up to 90 W m^{-3}, 104 W m^{-3} and current density of 30 A m^{-2}, respectively. However in practice, clogging problems due to suspended particles in real wastewater are likely to occur [16,17]. Applications such as wastewater treatment will require a continuous flow with high throughput, as well as high coulombic efficiency and COD removal. Helical electrode design geometries, with functionally three-dimensional electrode materials have been investigated in order to facilitate high throughput and provide structural integrity and to investigate performance with respect to operating conditions. Three-dimensional electrodes including reticulated vitreous carbon, granular activated carbon and multi-channel monolith carbon have been tested in the previous studies [18–20].

BES typically requires large electrode areas to increase the efficiency of bioelectrochemical reactions. It has been reported that the use of three-dimensional electrodes enabled higher power output compared to notionally two-dimensional or flat electrodes [15,21]. This is due to a higher surface-to-volume ratio which results in a higher population of bacteria attachment. Preparing large three-dimensional porous carbon electrodes with mechanically robust structures is a challenge, because excess levels of porosity reduce the mechanical properties of the material.

Design parameters are believed to be significant in determining the performance of BES, but to date there has been few studies which seek to investigate and differentiate the effects of topology, flow regime and materials. Preparation of large surface areas with micro and macro-porosity, for population by anode respiring microorganisms, may not in itself deliver higher performance. The optimization of multi-physical, chemical and biological variable needs ultimately to be considered, but the sensitivity of systems to such variables deserves further investigation.

In this paper, we develop two designs of helical electrodes using different carbon materials, namely; micro-porous monolithic conductive carbon (MMCC) produced using novel chemical synthetic methods, and layered carbon veil on a spoked former (LVSF), to investigate the concept of using the flow channel as a means of controlling the biofilm projected area and electrode spacing in a tubular MFC. The objectives of this study are to: a) compare the performance of two novel electrodes, which have been contrived to have comparable but different helical flow regimes and flow channels; carbon electrode materials and; surface characteristics and porosities, b) establish a helical flow channel concept in an MFC as a mechanism to increase shear induced mass transfer of substrate and products, and electrogenic biofilm formation, while maintaining near optimal component distribution in a tubular MFC, c) investigate the overall MFC performance variations due to temperature, substrate concentration and flow rate when operated in continuously fed mode. The empirical study is supported by computational fluid dynamics (CFD) modelling, which was conducted to investigate the effect of flow channel geometry on the flow regime, and to support the experimental results.

2. Materials and methods

2.1. MFC construction and operation

Replicate single MFC modules with air-cathode membrane electrode assemblies (MEAs) were fabricated, as reported previously [20], in all aspects apart from the anode assemblies. The module body (23 cm long and 4.0 cm diameter) was made from polypropylene tube. The MEA contained a cation exchange membrane (CMI-7000, Membrane International Inc., NJ, USA) and a carbon cloth cathode with 0.5 mg cm^{-2} Pt. The MFCs were operated in fed-batch mode with anaerobic digester sludge for 3 weeks during start up, then switched to continuous operation, during which different operating parameters were imposed; temperature, 25, 30, and 35 °C; substrate (acetate) concentration, 1, 10, 40 mM; and flow rate, 0.1, 2, 7.5 mL min^{-1}. During continuous operation, the liquid media containing acetate was delivered to the tubular reactors using an external peristaltic pump (Watson and Marlow, Falmouth, UK) for each MFC, setting and maintaining each flow rates listed above. During continuous operation, the media

reservoir was purged with nitrogen (99.9% v/v) to prevent oxygen contamination to the reactor.

2.2. Configuration of three-dimensional ABS frame for carbon veil

A 2-start helical former with spoked supports between the inside and outside diameters was produced using a rapid prototyping process from a CAD solid model using a Dimension 3D 1200es printer (Dimension Inc., MN, USA). The helical former was made from acrylonitrile butadiene styrene (ABS) plastic and provided a framework to accommodate layered carbon veil anode material (PRF Composite Materials, Dorset, UK), which followed the gap between fluid flow channels. The helical flow channel, which is flanked by spoked walls, had a minimum width of 5.4 mm and the mass of carbon veil lay in the helical channel to form the anode, was 6.4 g. The top layer of carbon wound into the channel was overlaid by a strip of fine stainless steel mesh of similar width (Type 304, Lenntech BV, Netherlands), to restrain and consolidate the carbon and simultaneously act as an electrical conductor/current collector for the anode carbon veil beneath (layered veil with spoked former, LVSF). This assembly is shown in Fig. 2b. Furthermore, the carbon veil acts as a porous support/electrode material for the attachment of electrochemically active bacteria for electricity generation. The helical geometry with intermittent spokes and carbon veil defined morphology/topology simultaneously increases the surface area available for bio-electrochemical reaction. The geometrical structure increases the mixing of the fluid and the associated mass transport of substrate and products into and out of the biofilm/electrode interface. The liquid volume of the MFC employing the LVSF electrode was 0.155 L.

2.3. Preparation of carbon monolith anode electrode

Hierarchically (fractal-like) porous carbon monoliths, with both meso- and macro-porosities, may be prepared using two polymers of different thermal stabilities, as precursor materials. For instance, polyfurfuryl alcohol (PFA) can be used as a carbon precursor that tends to carbonize at a high temperature while polyethylene (PE) as a thermally decomposable polymer which decomposes to gaseous products at a relatively low temperature under an inert atmosphere [22]. The two polymers can be mixed, pressed, cured and carbonized. The resulting structure can be made mechanically stable and produced into different shapes and sizes.

In order to prepare the 21.4 cm long and 3.6 cm diameter monolithic micro-porous conductive carbon (MMCC), the following method was used. A mixture of polyethylene (PE) powder (ultra-high molecular weight-surface modified, particle size 180 μm, Aldrich), polyfurfuryl alcohol (PFA) and a solution of oxalic acid (anhydrous, ≥99%, Fluka) in ethanol (96% GPR, VWR) was prepared. The volume ratio of PE to PFA was 12 to 1, which was adopted after various in-house experiments. The concentration of oxalic acid in the whole mixture was 0.25 mol L^{-1}. To prepare the PFA resin, furfuryl alcohol (98%, Aldrich) was mixed with a solution containing an equal volume of distilled water as the FA and sulphuric acid (98%, Aldrich), according to the literature [23]. Sulphuric acid acts as an initiator for polymerization of the furfuryl alcohol. The mixture was warmed up to 60 ± 2 °C over a water bath for 6 h, to achieve a sufficient level of polymerization with appropriate viscosity (7500 cP) for this application. Then, the mixture was pressed in a cylindrical mould (28 cm long and 5 cm diameter). After moulding, the samples were dried in an oven for 12 h at 90 °C. This step polymerized the PFA further and helped the hardening of the structure. Subsequently, samples were removed from the moulds, cured and carbonized at 150 and 1000 °C, respectively; under flowing nitrogen of 800 mL min^{-1}.

The curing and carbonization cycle is shown in Fig. 1a. As noted from the figure, the samples were heated from room temperature to 150 °C at a heating rate of 1 °C min^{-1} and were kept at this temperature for 4 h to complete the curing process. In order to carbonize the samples, these were further heated from 150 to 400 °C at a heating rate of 1 °C min^{-1} and from 400 to 600 °C they were heated very slowly (0.1 °C min^{-1}) to avoid rupture of the structure. This temperature range is the decomposition temperature range of polyethylene according to the data reported in the literature [24]. Subsequently, the samples were heated from 600 to 1000 °C at a heating rate of 1 °C min^{-1} and kept at 1000 °C for 2 h. After this heating cycle, the samples were impregnated with PFA at low viscosity (∼65 cP) and carbonized with the same cycle as above, to make the structure stronger. Impregnation of PFA into the carbon structures was facilitated by sonication of the samples in the low viscosity PFA for 1 h.

The conceptual, three dimensional anode architecture has been developed for use with the MFC modules described above. The helical channel was machined into the cylindrical monolithic carbon electrode using a numerically controlled milling machine equipped with rotating controlled chuck (EMCO PC-MILL 300, EMCO Maier G.m.b.H, Austria), which allowed the helix to be milled with comparable dimensions to the ABS former of the LVSF configuration. The liquid volume of the MFC employing the MMCC electrode was 0.150 L.

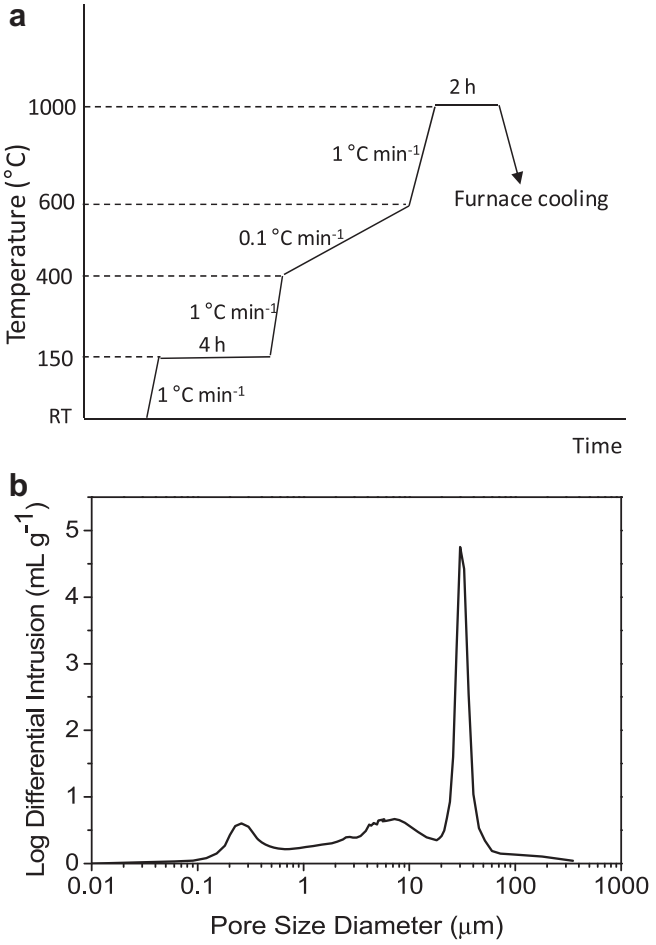

Fig. 1. (a) Schematic diagram of curing and carbonization cycle of the carbon monoliths, (b) Pore size diameter (μm) vs. Log differential intrusion (mL g^{-1}) of the carbon monolith.

2.4. Characterization of monolith carbon

A Jeol JSM 6300F field-emission scanning electron microscope (SEM) was used to characterize the structure and morphology of the carbon monoliths. Pore size distribution of the carbon structures was examined using a Micromeritics Mercury Intrusion Autopore-IV. Compressive strength of the monoliths was evaluated using an Instron 8500 testing machine with a loading rate of 0.5 MPa s^{-1}. Electrical resistivity of the monoliths was determined by a four-point technique using a Jandel four-point probing system. The macropore size range is between 0.15 and 60 μm with three peaks at 0.25, 6.5 and 29 μm and the majority of pores at 29 μm (Fig. 1b). Mechanical strength of the carbon monoliths was estimated by compression tests and found to be 2.6 ± 0.6 MPa. Electrical conductivity of the carbon structures was estimated by the four-point technique to be 8 ± 0.5 S cm^{-1}.

2.5. CFD methodology

Anode geometry was modelled using COMSOL Multiphysics (Comsol Ltd., Cambridge, UK) as shown in Fig. 7, with anode case and end caps with holes for the influent and effluent pipes in. The anode geometry model was half that of the physical anodes to reduce computational costs while still modelling fully developed flow in the study. The flow rates associated with the models matched the experimental conditions of 0.1, 2 and 7.5 mL min^{-1}. A notional Reynolds numbers for these flow rates were determined to be 17.81, 4.75 and 0.24 respectively, determining the characteristic length from the rectangular flow channel area of 5.4 mm × 10.3 mm, yielding an equivalent hydraulic diameter of 7.085 mm. Standard properties of water were used to represent the media fluid. Hence, laminar flow was considered in the investigation of the flow patterns at the surface (side wall) of the LVSF anode, where most of the bio-electrochemical activity is thought to reside.

Laminar, incompressible fluid flow with isotropic fluid (here, water) properties and no-slip wall conditions ($\mathbf{u} = 0$), were considered for the results presented. The analysis used an implementation of the Navier-Stokes equations: $\rho(\mathbf{u}\cdot\nabla)\mathbf{u} = \nabla\cdot[-p\mathrm{I} + \mu(\nabla\mathbf{u} + (\nabla\mathbf{u})^{\mathbf{T}})]$ and $\rho\nabla\cdot\mathbf{u} = 0$.

A tetrahedral mesh for fluid flow analysis was implemented and a 'parametric' flow rate study was performed for the three volumetric flow rates mentioned. The reactors were operated in continuous mode and steady state was assumed. Hence, stationary fluid flow conditions were studied to look at the flow patterns arising at the anode walls.

2.6. Electrochemical analyses

The voltage and current across the load and the temperature were monitored using a virtual instrument based data logging system (National Instruments, LabVIEW™) and a calibrated thermistor circuit connected to an analogue input on the I/O card respectively. The power output measurements were determined using potentiodynamic polarization (scan rate 10 mV s^{-1}) using a Solartron Electrochemical Interface (Farnborough, UK) controlled by dedicated software (CorrWare 2™, Scribner Associate Inc., NC). The power was calculated using the potential and current measured between the anode and cathode [25].

3. Results

A microscopic investigation of the electrodes and the biofilms developed thereon is presented. This is followed by performance results from the MFCs while subject to varying operating conditions; which is then augmented by results from comparable CFD simulation studies.

3.1. Three dimensional carbon structure and biofilm formation

Two different configurations of carbon structure were developed with carbon monolith (MMCC) and veil (LVSF), respectively (Fig. 2a and b). A near steady state pattern of liquid flow is established within the helical fluid channel of three-dimensional electrode structures. The biofilm formation on the different carbon materials is shown in Fig. 3b and d and compared to un-inoculated abiotic carbon materials (Fig. 3a and c). The microstructure of pores was covered by a thick biofilm and it was expected that this prevented mass transport between substrate in the bulk liquid and the internal surfaces and biofilm of the MMCC, thus reducing the bio-surface availability of the MMCC material (Fig. 3b).

By comparison, the LVSF carbon veil electrode consists of randomly matted carbon fibres (approximately 10 μm in thickness) which possess many micro-scale interstitial access paths. Therefore the influence of shear stress in the bulk liquid flow might effect flow into the internal space of the LVSF carbon material more significantly. The biofilm formation on the carbon veil electrode was relatively sparser; therefore the porosity was maintained on the surface even after the stable establishment of the biofilm. Thus the bulk liquid condition (i.e. concentration and shear) can more

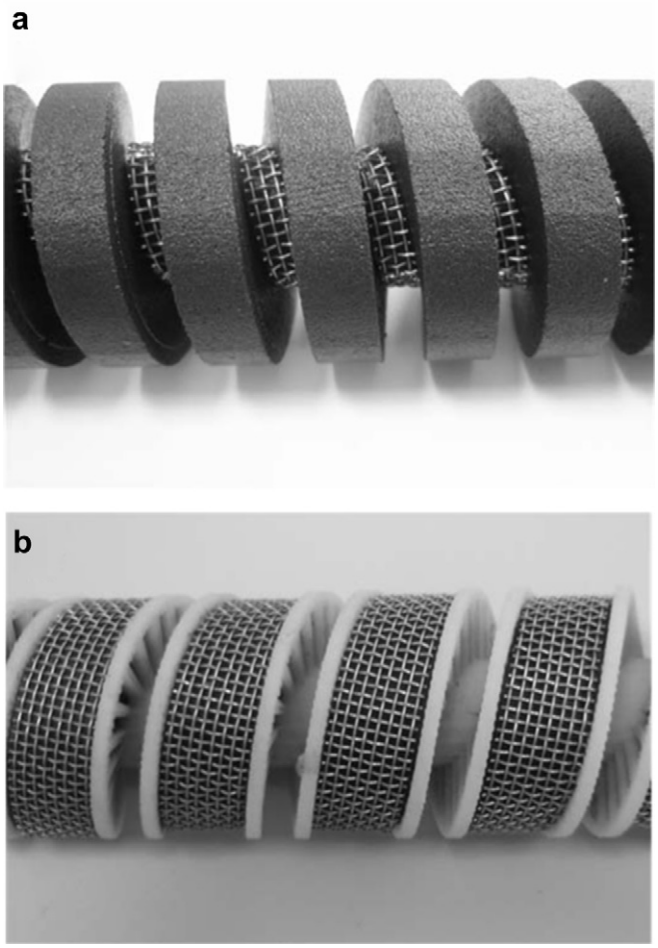

Fig. 2. Illustration of the anode electrodes tested: (a) Helical monolith carbon (MMCC) and (b) spoked carbon veil electrode assembly (LVSF), showing spokes on ABS plastic former.

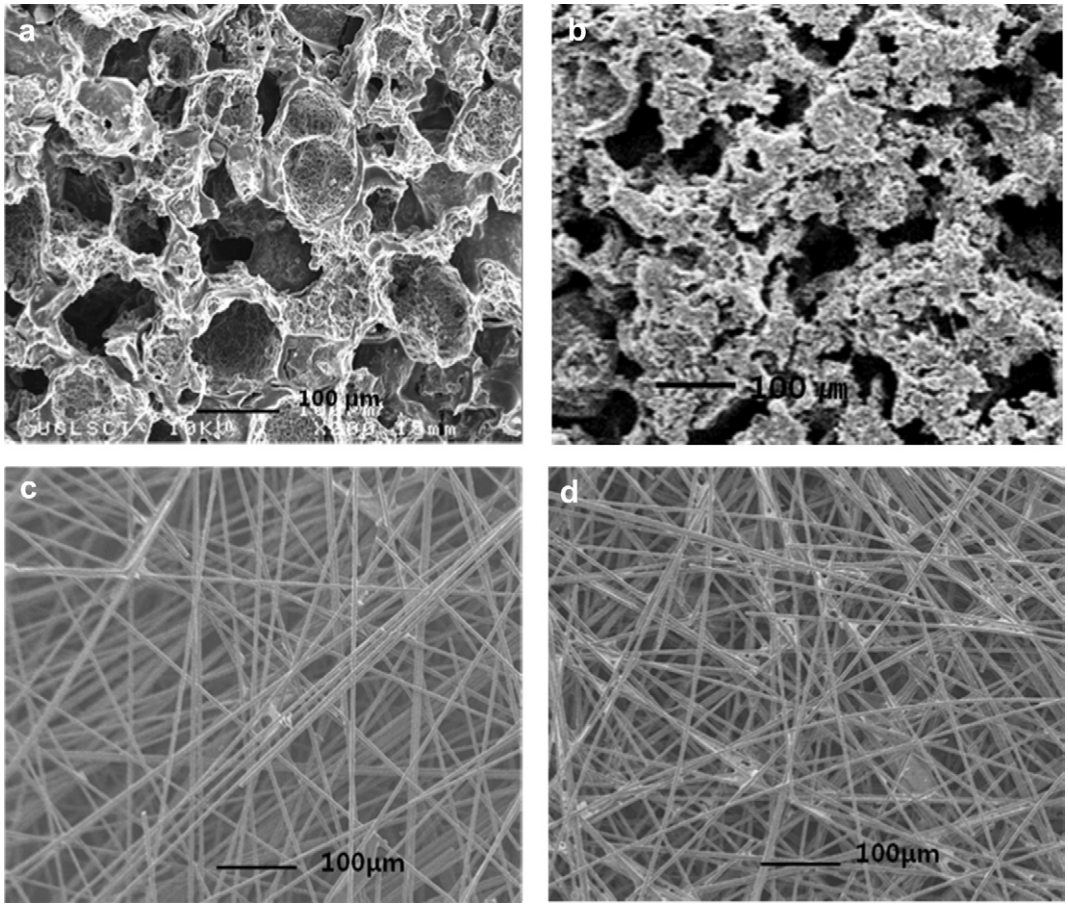

Fig. 3. Scanning electron microscopy images of (a) the abiotic carbon monolith (MMCC) after impregnation with PFA and before inoculation, (b) MMCC after biofilm formation, (c) the carbon veil electrode (LVSF) before inoculation and (d) LVSF after biofilm formation.

readily affect conditions deeper into the LVSF electrode porosity created by the carbon fibres than the MMCC, by diffusing and mixing of substrate and microbial products (including H^+ and carbonic acid and CO_2) in and out of the electrochemical reaction. The biofilm formation on the different carbon materials might affect the anode performance depending on operating conditions, particularly substrate concentration and flow rate.

3.2. Effect of acetate concentration

The maximum power production of tubular MFCs with carbon MMCC and LVSF electrodes was investigated at different acetate concentrations (1–40 mM) at 25 °C, initially in batch operation. The open circuit voltages (OCV) ranged between 0.45 and 0.49 V in both anode electrode configurations. The MMCC electrode showed an increase in maximum power (7.6 mW, 50.7 W m^{-3} based on empty bed space) at 10 mM of acetate while it decreased to 5.5 mW (36.6 W m^{-3}) at 40 mM and 2 mL min^{-1} (Fig. 4a). The power from the LVSF electrode, however gradually increase according to increases in acetate concentration; and did so more clearly as higher flow rates were applied (Fig. 4b). This result indicates that the increase in acetate concentration might not be correlated to increases in power, probably due to inefficient buffering capacity in the proximity of electrode. Thus localized pH increase may inhibit the electrochemical reactions. Lee et al. (2008) reported that buffering capacity significantly affects the potential in such systems [26]. Therefore bulk substrate concentration, porosity and surface morphology of electrode material/flow channel should be considered when optimizing for power production and other performance measures in MFCs.

3.3. Effect of temperature

Fig. 5 shows the effect of temperature on power production at different flow rates. The power production of the MMCC electrode increases over the range of temperatures tested (25–35 °C), when operated in both batch and continuous flow condition (0.1–2 mL min^{-1}); while power flattened out at 7.5 mL min^{-1} (Fig. 5a). The power production of the LVSF electrode shows similar trend, with power increasing according to temperature (Fig. 5b). When the cell was operated in continuous mode, the power from the LVSF system increased more clearly than the MMCC, to 3.1 mW from batch operation; and again at different flow rates as compared to the MMCC electrode. However, overall power performance of the LVFC was lower than the MMCC (9.4 mW at 2 mL min^{-1}). Increasing cell performance due to increasing operating temperature (in the range studied) may be rationalized in two respects in MFCs: Firstly, higher temperatures enhance the electrochemical reaction kinetics and metabolic activity of the catalyst, and secondly, by improving mass transport through increased molecular motion at the interface.

3.4. Effect of flow rate

The effect of flow rate on power production was investigated using flow rates from 0.1 to 7.5 mL min^{-1} (HRT 25 h–0.33 h), as

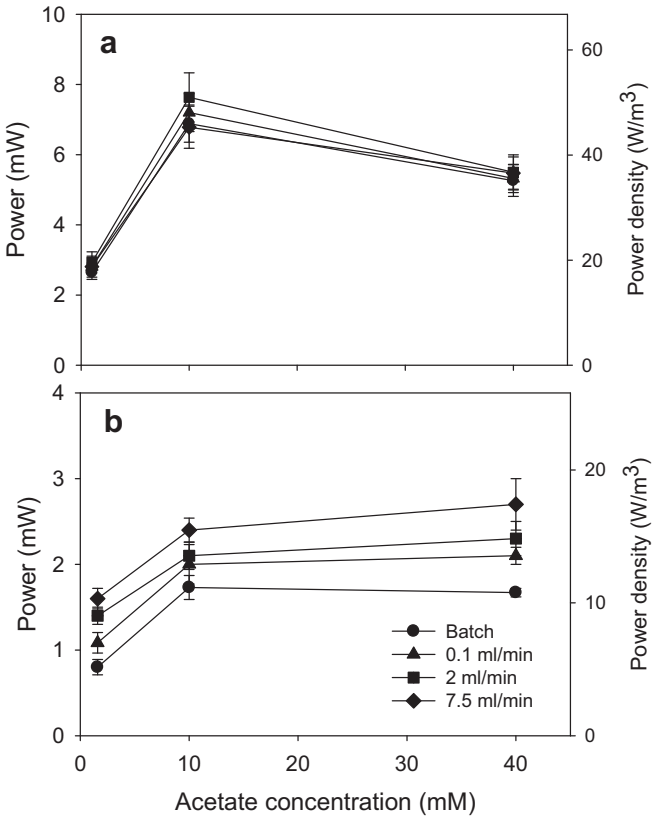

Fig. 4. Effect of concentration of acetate on maximum power density at 25 °C. (a) Helical monolithic carbon (MMCC), (b) spoked carbon veil electrode (LVSF).

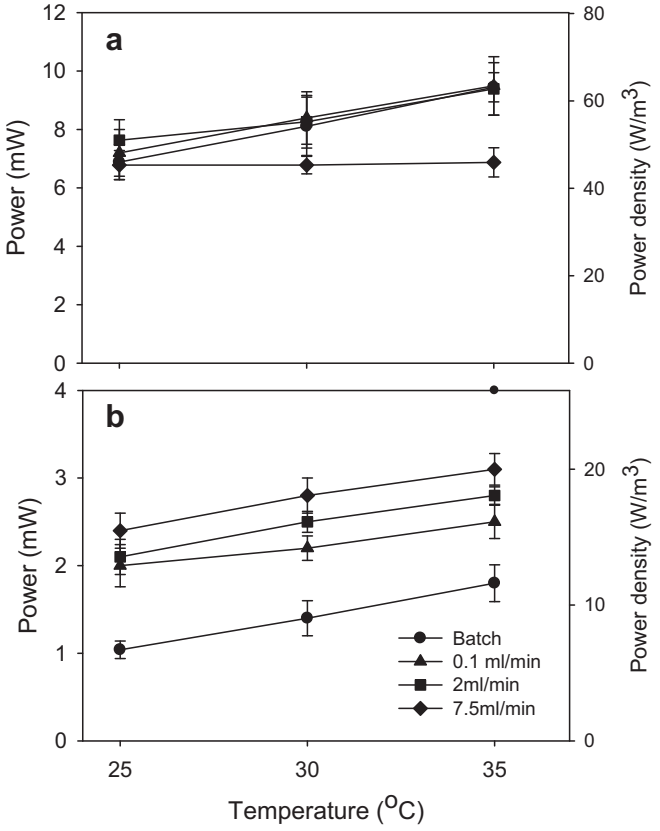

Fig. 5. Effect of temperature on maximum power at 10 mM acetate. (a) Helical monolith carbon (MMCC), (b) spoke carbon veil electrode (LVSF).

compared to batch condition. The MMCC electrode shows increased power when the operating condition was changed from batch to 0.1 mL min^{-1}. However, increases in flow rate did not result in further improvements in power production during continuous operation with flow rates between 0.1 and 7.5 mL min^{-1}. The power production of LVSF was lower than the MMCC in absolute terms. However, the power production of the LVSF showed an increase in the transition to continuous operation from batch, gradually increased to 2.7 mW (40 mM acetate), in response to flow rate increases. The trend in power increase was similar throughout the range of flow rates tested (0.1–7.5 mL min^{-1}), regardless of acetate concentration.

3.5. Computational fluid dynamics modelling of three-dimensional carbon electrodes

Model simulation results are presented as 3D velocity plots, where arrows show the direction of fluid particles and calibrated tones/colours, the magnitude. The helical flow channel is presented in detail by zooming in on typical areas of interest in order to visualize flow patterns in the vicinity of the flow/biofilm/carbon interfaces and between the spokes in LVSF electrode. As one may observe in arrow plots of Fig. 7a, the fluid velocity is $\sim 0.2 \times 10^{-4}$ m s^{-1} in the bulk and near the surface. When the flow rate increased (Fig. 7b and c), bulk fluid velocity increased to $\sim 1.0 \times 10^{-4}$ m s^{-1} and up to 1.4×10^{-4} m s^{-1}, and even higher velocities close to the surface. However, the direction of the flow (arrows) is aligned with the bulk, virtually homogeneous flow. This suggests that there is relatively little turbulence and/or mixing along the flow path. Therefore, little mixing (with associated mass transport) is evident in the component direction orthogonal to the liquid flow at the biofilm/electrode surface. Limited mixing does however occur at macro scale, resulting from boundary layer development and the twist in the helical path. Limited mixing may be one of the reasons why increases in flow rate did not show any significant increase in the power generation with the MMCC electrode, as shown in the previous section (Fig. 6a). Mixing is desirable in biological reactors where inhibitory metabolic products and reactants/substrate should be removed or supplied to microorganisms by various mechanisms. Without mixing or diffusion, a major proportion of the substrate would enter and leave the helical path un-altered. Likewise, without these mass transfer mechanisms and electro-migratory field effects, protons could pass to the effluent more readily. Increasing mixing, diffusion and proton-motive potentials will therefore be expected to enhance performance.

Comparing the arrow plots, Fig. 7d–f; it can be seen that increasing flow rate increases the fluid particles' velocity in localized areas from $\sim 0.2 \times 10^{-4}$ m s^{-1} up to ~ 0.6 m s^{-1} and ~ 1.4 m s^{-1} for higher flow rates. Interestingly but as expected, the LVSF spokes produce localized eddies and these rapidly accelerate fluid particles and are thought to have increased mixing and the turnover of the substrate and hence overall, power generation. An increase in the power generation was therefore evident when increased flow rate was imposed on this type of anode configuration (LVSF).

4. Discussion

Two different types of helical anode configurations with different but comparable channels, presented different flow patterns, which allowed the evaluation of the effect of substrate concentration, temperature and flow rate on biofilm formation and subsequent power output. Porous monolith carbon made from carbonaceous polymers in the MMCC showed higher power

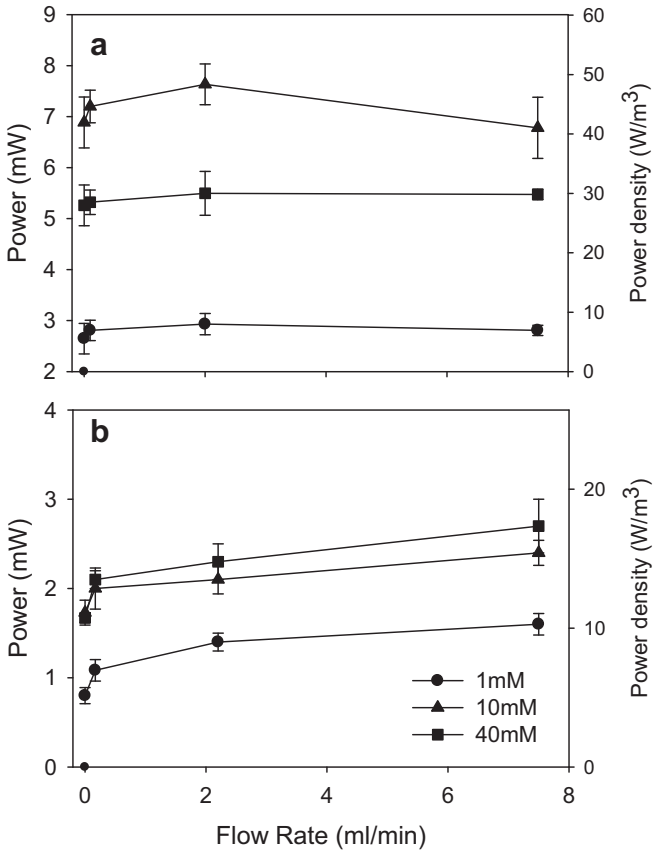

Fig. 6. Effect of flow rate on maximum power density. (a) Helical monolith carbon (MMCC), (b) spoke carbon veil electrode (LVSF).

performance than the carbon veil materials of LVSF in direct comparison. However, there were different responses in the power outputs from the two types of anode, in response to operational conditions, which indicated system design sensitivities related to induced shear, when the different anode electrodes were used in a longitudinal tubular MFC reactor configuration [27].

4.1. The helical flow channel concept

The use of a helical flow channel allows the cross sectional area available for fluid flow to be adjusted during design. Consequently the flow rate and related shear, mixing and mass transfer are also affected. The helical configuration will allow the liquid volume to surface ratio to be largely adjustable at the design stage; and so to the hydraulic retention time (HRT). At the same time the minimal separation between anode and cathode are maintained, so minimizing ohmic overpotential losses in the liquid phase. The performance of the helical anodes as tested has exceeded the performance of an earlier anode concept; a concentric cylindrical anode operated with the same arrangement of cathode assembly, as reported in e.g. [28].

In this study, the peak power was 1.4 mW, 6.2 W m^{-3}; compared to 9.5 mW at 45 mA (63.5 W m^{-3}) for the MMCC, based on empty bed volume. This is approximately a 10 fold increase over previous results, although the LVSF was less dramatic at 3.1 mW at 11 mA (20 W m^{-3}), with a 3 fold increase. It is expected that this power density can be increased for both MMCC and LCSF by maximizing the area to volume ratio. However, the direct comparison of power with previous results requires the *caveat lector* in that a potentiodynamic method using a relatively fast scan rate (e.g. 10 mV s^{-1}) tends to over-estimate the power production in comparison to near-static power measurements used previously. Therefore the method is more useful for comparing the two electrode configurations with their respective materials, and the operational parameters, as the potentiodynamic method was used on both.

4.2. Shear in fluid flow and biofilm formation

MFCs typically require an exoelectrogenic biofilm on the anode electrode, which is developed from a suspended community, naturally and by adaptation in electrogenic condition. Our results show that the biofilms were developed densely within a relatively shallow penetration of the MMCC electrode; therefore the inner micro-porous volume may not be effectively utilized for bacterial attachment and bioelectrochemical activity [10]. In the LVSF electrode, the biomass development, estimated by DNA concentration has been shown to have most of the biofilm biomass on the outer layer of the veil, rapidly decreasing as its depth from the surface increases (data not shown). This indicates that access to substrate, governed partially by pore size and spatial distribution of the electrode, are (along with ohmic losses, and mass transfer), amongst the most important factors affecting MFC performance, rather than absolute measures of surface area.

It has been reported that shear stress and hydrodynamic conditions in bacterial media influence the composition of the microbial communities, can slow down biofilm maturation and tend to maintain an electroactive biofilm [8,13]. The effect of shear stress on the biofilm's physical characteristics and electrochemical activity may be explained by physiological adaptation mechanisms in electrogenic species which use electrodes as final electron acceptor. Fluid dynamic forces provide selection pressure on the microbial ecology of the biofilm, favouring intimate and firm contact between biofilm and electrode. An investigation of the cell viability as a function of depth within porous media would be necessary to evaluate the efficiency and design of MMCC electrodes.

4.3. Operational parameters: substrate concentration, temperature, and HRT and flow rate in MFC

Bioelectrochemical reactions in electrogenic biofilms are governed by operating conditions such as temperature, availability and concentration of substrate and its (mass) transport into the biofilm/electrode, induced by flow rate and shear stress. MFC performance, as stated, is directly affected by temperature [11], but the performance may be time and substrate dependent and can influence electrode biofilm formation [12,29]. Ieropoulos et al. reported the effect of flow rate on biofilm formation and consequent power production [9]. In this paper, they found increased flow rate decreased power density, which they attributed to oxygen ingress at high flow rate since an increase in dissolved oxygen inhibits electrogenesis [30]. In our results, a decrease of power was obtained at high flow rate (7.5 mL min^{-1}) with the MMCC electrode, even when using nitrogen purging to exclude oxygen contamination in the feed. This compared to the reverse trend in the LVSF electrode, which showed a gradual increase at the higher flow rates. We deduce and expect that this would result from the different (*c.f.* MMCC) surface morphology of the electrode. The LVSF effectively has flow disrupting stepped walls, as illustrated in Fig. 2, which induce mixing. The effect of HRT on MFC performance has been investigated in previous studies [24,26,27]. However, it was not extensively studied in the context of such porous electrodes and hydrodynamic flow effects, or biofilm formation on the electrode surfaces. The pumping costs and energy required to increase flow rate and shear stresses should be considered when MFCs/BES are to

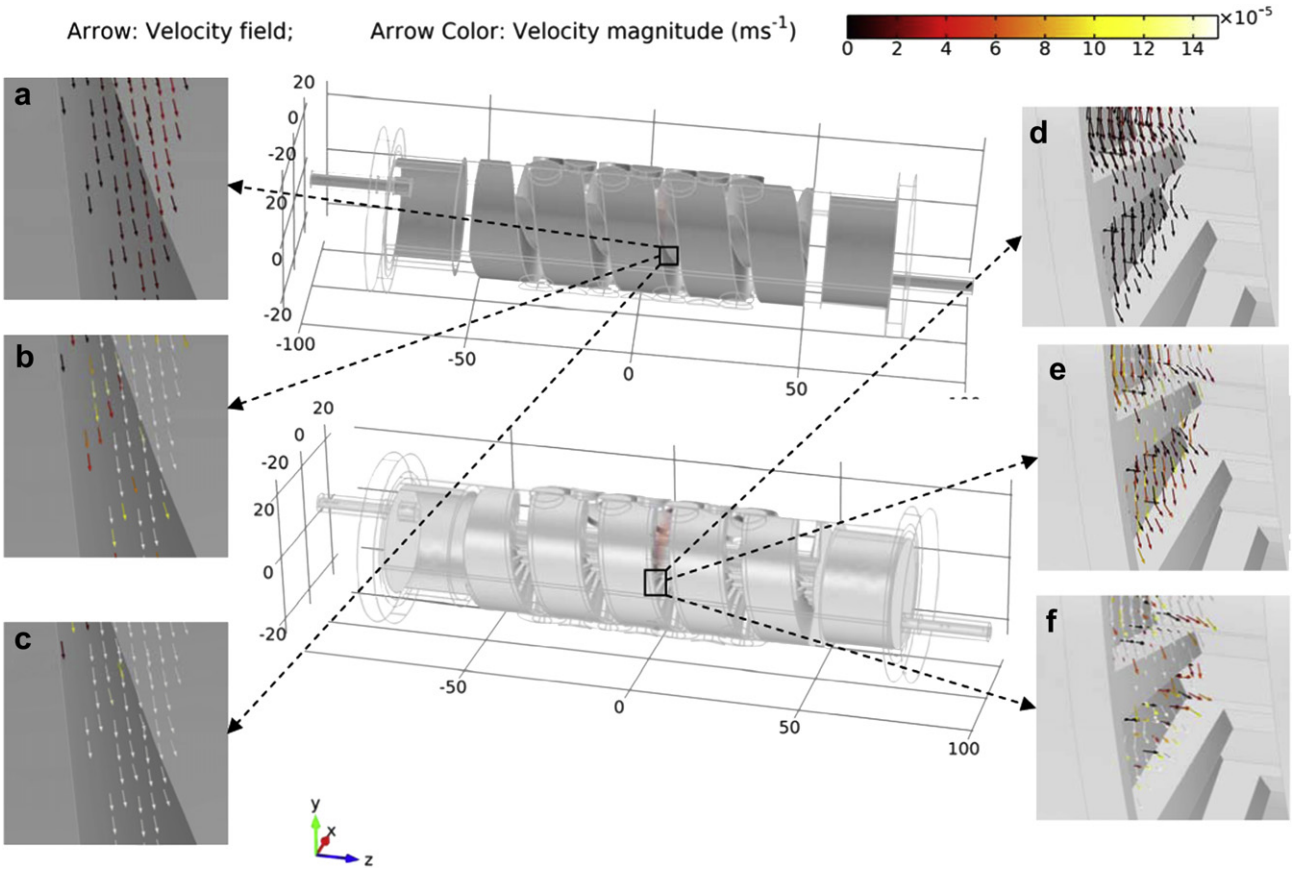

Fig. 7. 3D arrow plots showing fluid particle velocities (with arrows showing velocity field direction and their tone indicates magnitude); zoomed in on helical flow path of monolith micro-porous conductive carbon (MMCC) (a)–(c); and layered veil with spoked former (LVSF) (d)–(f). Inlet velocities and flow rates (a, d) V_{in} = 1.67e − 9 $m^3\ s^{-1}$ [0.1 mL min^{-1}], (b, e) 3.33e − 8 $m^3\ s^{-1}$ [2 mL min^{-1}], (c, f) 1.25e − 7 $m^3\ s^{-1}$ [7.5 mL min^{-1}].

be deployed in wastewater treatment or other processes which will be assessed in part by energy recovery.

4.4. Reducing mass transfer limitations

In order to overcome mass transport limitations in porous electrodes, diffusive mass transfer mechanisms need to be augmented by a forced convective or invective mass transfer shear related mixing. Such mixing alleviates current density limitations caused by substrate supply and product inhibition and so increase power density. The MMCC electrode shows significantly higher power production than the LVSF electrode (9.5 mW compared to 3.1 mW, respectively). However, the effect of flow-rate change was different in each case. A key difference lies in the different fluid dynamic flow patterns within the flow channel of each electrode. Optimizing the flow path geometry to balance induced mixing against pressure losses through the flow path, while seeking to maximize net power production and substrate oxidation, would reduce the mass transfer limitations. Also, optimization of the micro/macro structure of the electrode in terms of the size and distribution of pores (available biofilm surface landing) should be considered for specific ranges of operating conditions. However, as has been seen in this study, the electronic conductivities of the electrode materials can have a substantial effect on the absolute performance of the system. The MMCC displayed higher power generation in part due to higher electronic conductivity than the LVSF, and clearly, the same would be true of any other overpotential losses in the system.

Cathode limitations might affect the overall performance of the systems. In this study however, the cathodic performance was effectively excluded from the experimental investigation by using replicated cathodes of comparable performance. Membrane electrode assemblies employing an air-cathode have advantages with regard to scale-up, in the tubular MFC systems employed. Air cathodes are expected to reduce operating and capital costs incurred in the aeration and circulation of catholyte. Cathode catalyst deactivation by biomass contamination may also occur in wet-cathodes and dual chamber systems [15,30]. A single chamber reactor design may yield simplicity and therefore facilitate cost effective scale-up. However, improvements in the cathode system of longitudinal tubular reactors will be required to reduce the limitations introduced by the cathode.

4.5. Implication for scale-up

The scalability of the anodic systems requires consideration, but is not independent of other system elements. BES may be applied to wastewater treatment, formation of product, power generation or other applications; operating condition may vary greatly, and all these considerations may affect design details and hence the plausibility of scale-up. Temperature and flow regimes may contribute to maximizing energy recovery and conversion efficiency and warrant further study in such systems, particularly where parasitic power consumption could seriously affect industrial applicability. The results we obtained from two comparable but different electrode materials suggest the methods can provide

useful procedures to generate design data for such electrically conductive biocatalyzed electrodes. Importantly, near optimal operating conditions may also be determined, which should lead to enhanced system applicability in industrial environments.

Acknowledgement

This research was funded by the RCUK Energy Programme, SUPERGEN Biological Fuel Cell project (EP/D047943/1) supported by grant 68-3A75-3-150. The Energy Programme is an RCUK cross-council initiative led by EPSRC and contributed to by ESRC, NERC, BBSRC and STFC.

References

[1] S.T. Oh, J.R. Kim, G.C. Premier, T.H. Lee, C. Kim, W.T. Sloan, Biotechnol. Adv. 28 (2010) 871–881.
[2] B.E. Logan, Microbial Fuel Cells, Wiley-Interscience, Hoboken, N.J, 2008.
[3] K. Rabaey, G. Lissens, W. Verstraete, in: Biofuels for Fuel Cells: Biomass Fermentation Towards Usage in Fuel Cells, IWA Publishing, London, 2005.
[4] D. Singh, D.M. Lu, N. Djilali, Int. J. Eng. Sci. 37 (1999) 431–452.
[5] U. Pasaogullari, C.Y. Wang, J. Electrochem. Soc. 151 (2004) A399–A406.
[6] C.I. Torres, A.K. Marcus, B.E. Rittmann, Biotechnol. Bioeng. 100 (2008) 872–881.
[7] H. Moon, I.S. Chang, J.K. Jang, B.H. Kim, Biochem. Eng. J. 27 (2005) 59–65.
[8] H.T. Pham, N. Boon, P. Aelterman, L. Clauwaert, D. Schamphelaire, P.v. Oostveldt, K. Verbeken, K. Rabaey, W. Verstraete, Microb. Biotechnol. 1 (2008) 487–496.
[9] I. Ieropoulos, J. Winfield, J. Greenman, Bioresour. Technol. 101 (2010) 3520–3525.
[10] C. Picioreanu, M.C.M. van Loosdrecht, T.P. Curtis, K. Scott, Bioelectrochemistry 78 (2010) 8–24.
[11] S.A. Patil, F. Harnisch, B. Kapadnis, U. Schroder, Biosens. Bioelectron. 26 (2011) 803–808.
[12] I.S. Michie, J.R. Kim, R.M. Dinsdale, A.J. Guwy, G.C. Premier, Appl. Microbiol. Biotechnol. 92 (2011) 419–430.
[13] A. Rochex, J.J. Godon, N. Bernet, R. Escudie, Water Res. 42 (2008) 4915–4922.
[14] J.R. Kim, N. Rahunen, J. Varcoe, R.M. Dinsdale, A.J. Guwy, A. Thumser, R.C. Slade, C. Avignone-Rossa, G.C. Premier, Appl. Microbiol. Biotechnol. 90 (2011) 1179–1191.
[15] K. Rabaey, P. Clauwaert, P. Aelterman, W. Verstraete, Environ. Sci. Technol. 39 (2005) 8077–8082.
[16] P. Aelterman, M. Versichele, M. Marzorati, N. Boon, W. Verstraete, Bioresour. Technol. 99 (2008) 8895–8902.
[17] S. Chen, H. Hou, F. Harnisch, S.S. Patil, A.A. Carmona-Martinez, S. Agarwal, Y. Zhang, S. Sinha-Ray, A.L. Yarin, G. Andreas, U. Schroder, Energy Environ. Sci. 4 (2011) 1417–1421.
[18] Z. He, S.D. Minteer, L.T. Angenent, Environ. Sci. Technol. 39 (2005) 5262–5267.
[19] Z. He, N. Wagner, S.D. Minteer, L.T. Angenent, Environ. Sci. Technol. 40 (2006) 5212–5217.
[20] J.R. Kim, G.C. Premier, F.R. Hawkes, R.M. Dinsdale, A.J. Guwy, J. Power Sources 187 (2009) 393–399.
[21] D. Sell, P. Krämer, G. Kreysa, Appl. Microbiol. Biotechnol. 31 (1989) 211–213.
[22] N. Amini, K.F. Aguey-Zinsou, Z.X. Guo, Carbon 49 (2011) 3857–3864.
[23] M. Chanda, S.R. Dinesh, Angew. Makromol. Chem. 69 (1978) 85–98.
[24] D. Jinno, A.K. Gupta, K. Yoshikawa, Environ. Eng. Sci. 21 (2004) 65–72.
[25] C. Donovan, A. Dewan, H. Peng, D. Heo, H. Beyenal, J. Power Sources 196 (2011) 1171–1177.
[26] H.-S. Lee, M.B. Salerno, B.E. Rittmann, Environ. Sci. Technol. 42 (2008) 2401–2407.
[27] J.R. Kim, J. Rodriguez, F.R. Hawkes, R.M. Dinsdale, A.J. Guwy, G.C. Premier, Energy Environ. Sci. 4 (2011) 459–465.
[28] J.R. Kim, G.C. Premier, F.R. Hawkes, J. Rodríguez, R.M. Dinsdale, A.J. Guwy, Bioresour. Technol. 101 (2010) 1190–1198.
[29] I.S. Michie, J.R. Kim, R.M. Dinsdale, A.J. Guwy, G.C. Premier, Energy Environ. Sci. 4 (2011) 1011–1019.
[30] S.E. Oh, J.R. Kim, J.H. Joo, B.E. Logan, Water Sci. Technol. 60 (2009) 1311–1317.